First-principles study of structural, elastic, and electronic properties of M23C6 and MC carbides (M = Ru, Rh, Pd, Os, Ir, and Pt)

ARTICLE *in* PHYSICA STATUS SOLIDI (B) · JANUARY 2014

Impact Factor: 1.49 · DOI: 10.1002/pssb.201349062

2 AUTHORS, INCLUDING:

Nadezhda I Medvedeva

Russian Academy of Sciences

159 PUBLICATIONS **1,409** CITATIONS

SEE PROFILE

Phys. Status Solidi B **251,** No. 1, 148–154 (2014) / **DOI** 10.1002/pssb.201349062

physica status solidi b
www.pss-b.com
basic solid state physics

First-principles study of structural, elastic, and electronic properties of $M_{23}C_6$ and MC carbides (M = Ru, Rh, Pd, Os, Ir, and Pt)

N. I. Medvedeva and A. L. Ivanovskii*

Institute of Solid State Chemistry, Ural Branch, Russian Academy of Sciences, Pervomaiskaya St. 91, Ekaterinburg 620990, Russia

Received 13 February 2013, revised 9 July 2013, accepted 19 July 2013
Published online 19 August 2013

Keywords elastic properties, first-principles calculations, mechanical stability, metal carbides

* Corresponding author: e-mail ivanovskii@ihim.uran.ru, Phone: +7(343)374533, Fax: ++7(343)3744495

Using first-principles calculations within the density functional theory we studied the electronic structure, elastic properties, and stability of $M_{23}C_6$ carbides, where M are the platinum-metals: Ru, Rh, Pd, Os, Ir, or Pt. The lattice constants, elastic parameters, formation energies, and densities of states of $M_{23}C_6$ were compared with those for mono-carbides MC. We demonstrated that these carbides have the positive formation energies and predicted the mechanically stable phases. We found that $M_{23}C_6$ carbides are energetically more favorable than the corresponding MC carbides due to the stronger M–M interactions in $M_{23}C_6$.

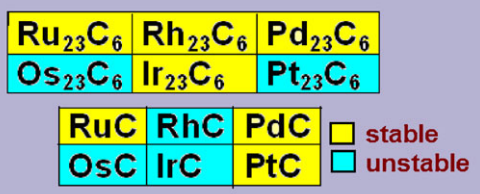

Mechanically stable and unstable $M_{23}C_6$ and MC carbides.

1 Introduction For a long time it was assumed that the platinum group metals (M = Ru, Rh, Pd, Os, Ir, and Pt) cannot form stable phases with carbon [1, 2]. The successful high-pressure and high-temperature synthesis of platinum carbide by Ono et al. [3] (cubic PtC_x; space group $Fm3m$; lattice constant $a = 4.470$–4.814 Å, as depending on the external pressure) stimulated much activity in the development of new related platinum-metal carbides and in exploring of their properties. The obtained achievements in synthesis and simulation of these materials were reviewed recently in Refs. [4, 5].

The most exciting expectations of novel functionalities of these materials were related with their enhanced mechanical properties, and, in particular, with high micro-hardness and ultra-incompressibility. Already in the pioneering work [3], a high bulk modulus of the synthesized PtC was reported ($B \sim 301 \pm 15$ GPa), and then in the theoretical works (see Refs. [6–15] and references therein) the bulk modules and the Vickers hardness H_V were predicted for the MC phases. The value $H_V \sim 42.8$ GPa was obtained for zinc-blende (ZB) RuC [6] and this carbide should belong to the class of superhard materials having the Vickers hardness >40 GPa [16].

One of the central issues for the platinum-metal carbides concerns the interplay between their stoichiometry, structure, stability, and properties. For mono-carbides MC, the competing crystal structures such as rocksalt ($B1$), cesium chloride ($B2$), ZB ($B3$), wurtzite ($B4$), nickel-arsenide ($B8$), tungsten carbide (WC) were discussed [4]. Attempts were made to understand the influence of stoichiometry and the M/C ratio on the stability of these carbides. The carbon-rich phases (M/C < 1) such as M_2C_3 and MC_2 (M = Os, Ir) were simulated theoretically [17, 18], but as far as we know, no experimental evidences for such phases are available now.

The formation of metal-rich phases (M/C > 1) seems to be more realistic, since the majority of the known mono-carbides of 3d–5d metals from Groups IVa–Va have a wide homogeneity range from MC to $MC_{0.50}$ owing to carbon vacancies, whereas metal-rich carbides, such as $M_{23}C_6$, M_7C_3, M_3C_2, M_2C, or M_3C may be formed in the related systems consisting of carbon and 3d metals from Groups VIa–VIIIa [2, 19, 20]. Recently, the properties of sub-stoichiometric carbides M_4C_3, M_2C, M_3C, and M_4C (M = Rh, Ir, Pd, and Pt) were simulated in [13, 18, 21], where the model structures (Ir_4Ge_3, anti-CaF_2, anti-ReO_3,

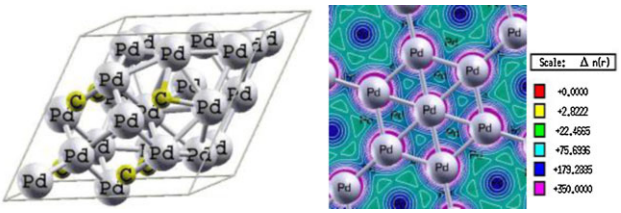

Figure 1 Atomic structure of γ-carbide $Pd_{23}C_6$ and charge density map, which illustrates the formation of atomic-like Pd–Pd bonds in this phase.

and Fe_4N structural types) were considered for the metal-rich carbides.

In the present work, we employed the first-principles calculations to study the trends in structural, elastic, and electronic properties of $M_{23}C_6$ carbides (M/C ∼ 3.83, M = Ru, Rh, Pd, Os, Ir, and Pt) with a face-centered cubic structure, see Refs. [22, 23]. This structural type (Fig. 1) was found for the so-called γ-carbides of 3d metals from Groups VIa–VIIIa.

The γ-carbides were formed during heat treatment by transformation of carbides with a low M/C ratio or from solid solutions. These carbides were observed in carbon steels with Cr, Mn, W, Mo, or V additions. The formation of $Cr_{23}C_6$, $Mn_{23}C_6$, or $(Cr,Fe)_{23}C_6$ precipitates is believed to affect the mechanical properties of alloys. Here we calculate also the formation energies of $M_{23}C_6$ carbides, where M is a platinum group metal, and discuss their stability in comparison with the well-studied cubic MC carbides.

2 Computational details The calculations were performed by using the density functional theory (DFT) as implemented in the Vienna *ab initio* simulation package (VASP) in the projector augmented waves (PAW) formalism [24, 25]. Exchange and correlation were described by generalized-gradient approximation (GGA) in the PBE parametrization [26]. We used a *k*-mesh of $12 \times 12 \times 12$ in calculations for mono-carbides and a $8 \times 8 \times 8$ *k*-point sampling grid was chosen for the $M_{23}C_6$ carbides. The valence electron density is defined by the four electrons for carbon ($2s^2$, $2p^2$) and s^1d^n electrons for platinum metals (s^1d^7 for Ru and Os, s^1d^8 for Rh and Ir, s^1d^9 for Pd and Pt). The kinetic energy cutoff of 350 eV was used to expand the valence orbitals into plane wave basis sets. We used the Methfessel–Paxton smearing for partial occupancies, which provides a very accurate description of the total energy for metals [27]. The smearing parameter σ depends on the density of states near the Fermi level and we took $\sigma = 0.2$ eV for all $M_{23}C_6$ carbides except of M = Pd and Pt, where $\sigma = 0.4$ eV [27]. The atomic relaxation was performed by minimizing the Hellmann–Feynman forces up to 0.01 eV Å^{-1} over all atoms. The elastic constants were calculated (version VASP5.2) by performing the finite distortions of lattice and deriving the elastic constants from the strain–stress relationship [28].

The $M_{23}C_6$ carbides crystallize in the cubic structure (space group $Fm\bar{3}m$) with four formula units ($Z = 4$) per a unit cell, where the metal atoms are placed in four crystallographic positions: *M*1 (4*a*), *M*2 (8*c*), *M*3 (32*f*), and *M*4 (48*h*), while carbon atoms occupy (24e) position [22, 23]. The rocksalt (*B*1) structure was considered for the mono-carbides MC. We optimized the lattice parameters for both MC and $M_{23}C_6$ as well as the internal coordinates for *M*3, *M*4 and C atoms in $M_{23}C_6$.

3 Results and discussion

3.1 Structural properties The optimized lattice parameters for the $M_{23}C_6$ and MC phases are listed in Table 1 in comparison with available experimental and theoretical data. We find our data for *B*1-MC to be in reasonable agreement with previous results. For $M_{23}C_6$, we predict that the lattice parameter *a* increases in the series $Ru_{23}C_6 \rightarrow Rh_{23}C_6 \rightarrow Pd_{23}C_6$ and $Os_{23}C_6 \rightarrow Ir_{23}C_6 \rightarrow Pt_{23}C_6$. This trend correlates with the atomic radii of platinum-metals R^{Ru} (1.34 Å) ∼ R^{Rh} (1.34 Å) < R^{Pd} (1.37 Å) and R^{Os} (1.35 Å) ∼ R^{Ir} (1.35 Å) < R^{Pt} (1.38 Å). The same trend was obtained in our calculations for the lattice parameters of *B*1-MC carbides, Table 1. The internal coordinates of nonequivalent atoms in $M_{23}C_6$ depend only slightly on the d metal (the fractional coordinates are 0.380, 0.333, and 0.279 for *M*3, *M*4, and C atoms in $Ru_{23}C_6$) and do not differ greatly from the observed values for $Cr_{23}C_6$, where these coordinates are 0.385, 0.330, and 0.275 for *M*3, *M*4 and C atoms, respectively. For $M_{23}C_6$, the unit cell volume per atom is larger by ∼17–20% than that for $Cr_{23}C_6$

Table 1 Lattice parameters (*a*, in Å) and cell volumes (*V*, in Å^3 atom^{-1}) for γ-carbides $M_{23}C_6$ and mono-carbides MC in comparison with available data.

carbides	*a*	*V*
$Ru_{23}C_6$	11.232	12.22
RuC	4.323 (4.37[a]; 4.236/4.327[b]; 4.444[c]; 4.26/4.31[d])	10.10
$Rh_{23}C_6$	11.338	12.57
RhC	4.357 (4.344[e]; 4.602[c]; 4.29/4.36[d])	10.34
$Pd_{23}C_6$	11.590	13.42
PdC	4.440 (4.428[c]; 4.430[b]; 4.439[f]; 4.444[c]; 4.36/4.44[d])	10.94
$Os_{23}C_6$	11.374	12.68
OsC	4.362 (4.308/4.361[g])	10.37
$Ir_{23}C_6$	11.464	12.99
IrC	4.405 (4.399[e])	10.68
$Pt_{23}C_6$	11.743	13.96
PtC	4.476 (4.470[e]; 4.506[b]; 4.403[f]; 4.51[h])	11.21

Available results are given in parentheses.
[a]Ref. [7], FP-LMTO;
[b]Ref. [12], PW-LDA/LAPW-GGA;
[c]Ref. [9], PW-GGA;
[d]Ref. [11], VASP, LDA/GGA;
[e]Ref. [13], FLAPW-GGA;
[f]Ref. [14], FLAPW-GGA;
[g]Ref. [15], VASP, LDA/GGA;
[h]Ref. [10], ABINIT-GGA.

($10.17\,Å^3\,atom^{-1}$ [22]), and for the platinum-metal MC carbides, Table 1. For the mono-carbides, the M–M and M–C distances (2.16 Å for RuC) are smaller than those for γ-carbides (for $Ru_{23}C_6$, they vary within 2.53–3.11 and 2.21–2.26 Å, respectively). We find that the average M–M distance in γ-carbides (2.78 Å in $Ru_{23}C_6$) is much closer to the M–M distance in the elemental metals (2.66 Å in hcp Ru) than in the monocarbides (2.16 Å for RuC), that suggests stronger M–M bonds in the $M_{23}C_6$ carbides.

3.2 Stability Certainly, one of the central issues for the proposed $M_{23}C_6$ phases concerns their relative stability. Such a prediction may be made in terms of the formation energy E_{form}, when we compare the energy of an examined phase E_{tot} and the energies of the constitutive simple species, namely, pure metals $E_{tot}(M)$ and graphite $E_{tot}(C^g)$ as the most stable allotrope of carbon. According to the formal reactions $M_{23}C_6 \rightarrow 23M + 6C$ and $MC \rightarrow M + C$, the values of E_{form} were calculated as $E_{form}(M_{23}C_6) = [E_{tot}(M_{23}C_6) - 23E_{tot}(M) - 6E_{tot}(C^g)]$ and $E_{form}(MC) = [E_{tot}(MC) - E_{tot}(M) - E_{tot}(C^g)]$, respectively. Note that within this definition a negative E_{form} indicates that it is energetically favorable for given reagents to form a stable phase, and vice versa. It should be also noted that all calculations were performed at 0 K, while the vibrational, entropy, and pressure effects were neglected.

We found that the formation energies for all the studied $M_{23}C_6$ and MC carbides are positive, see Fig. 2. This means that these carbides are meta-stable and their synthesis requires special thermodynamic conditions, for example, high pressures and enhanced temperatures, as in the case of PtC_x [3].

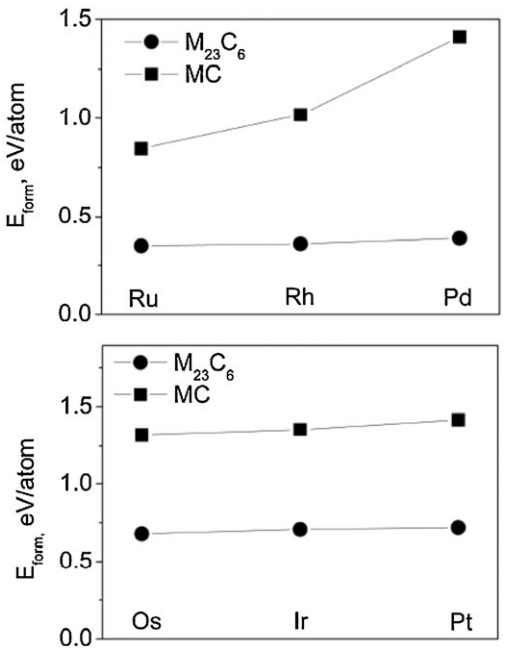

Figure 2 Formation energies of $M_{23}C_6$ and MC carbides, where M = Ru, Rh, Pd, Os, Ir, and Pt.

According to our calculations, $E_{form}(M_{23}C_6) < E_{form}(MC)$ and the formation of $M_{23}C_6$ phases is energetically more favorable as compared with the mono-carbides. In turn, $E_{form}(M_{23}{}^{4d}C_6) < E_{form}(M_{23}{}^{5d}C_6)$, i.e., the γ-carbides of Ru, Rh, and Pd are more stable than γ-carbides of Os, Ir, and Pt. The value of E_{form} for $M_{23}C_6$ depends weakly on the type of 4d or 5d metals as opposed to the mono-carbides of 4d metals, for which E_{form} increases sharply as going from RuC to PdC, Fig. 2. For all the examined $M_{23}C_6$ and MC carbides, their stability decreases over the transition metal series that can be understood from the filling of their d-like bands, see below.

To estimate the contribution of M–M and M–C bonds to the cohesive properties of $M_{23}C_6$ and MC, we followed the approach [29–34], where the total energy calculations were performed for the complete and partly empty sublattices of borides and carbides. We calculated the formation energies for hypothetical phases with empty carbon sites (X) – $M_{23}MX_6$ and MX at the same $M_{23}C_6$ and MC structures. For ruthenium carbides, we found E_{form} to be equal to +0.45 and +1.37 eV atom^{-1} for $M_{23}X_6$ and MX, respectively. By comparing these values with E_{form} for the complete carbides (+0.35 and +0.84 eV atom^{-1} for $Ru_{23}C_6$ and RuC, respectively) we show that the absence of carbon in $M_{23}C_6$ changes E_{form} only slightly, whereas it contributes strongly to destabilization of MC. Thus, we can conclude that the M–C bonds are weak and the M–M bonding determines the cohesion in $M_{23}C_6$, while the M–C bonds play an important role and give a large stabilizing contribution in MC carbides. The charge density map demonstrates the formation of the M–M bonds in $Pd_{23}C_6$ as example, Fig. 1.

3.3 Elastic properties In this section we discuss the elastic properties of $M_{23}C_6$ carbides in comparison with those for mono-carbides MC. Here the conventional "volume-conserving" technique was used in the calculation of stress tensors on strains applied to the equilibrium structure to obtain the elastic constants (C_{ij}), see review [16] for details. In this way the values of three independent elastic constants in the cubic symmetry (C_{11}, C_{12} and C_{44}) were estimated, Table 2.

We examined the conditions of intrinsic stability of $M_{23}C_6$ and MC carbides, when the Gibbs free energy of a phase is in a local minimum with respect to small structural deformations. In terms of elastic constants C_{ij}, this stability criterion (so-called mechanical stability) for cubic crystals [41] requires $(C_{11} - C_{12}) > 0$; $(C_{11} + 2C_{12}) > 0$; and $C_{44} > 0$. Such crystals are characterized by positive values of the bulk modulus B, shear modulus G and tetragonal shear modulus $G' = (C_{11} - C_{12})/2$. We found that only three MC carbides (RuC, PdC, and PtC) and four $M_{23}C_6$ carbides ($Ru_{23}C_6$, $Rh_{23}C_6$, $Pd_{23}C_6$, and $Ir_{23}C_6$) have elastic constants, which satisfy all of the aforementioned conditions, and these materials are supposed to be mechanically stable, Fig. 3. For all other phases $C_{44} < 0$ and we predict them to be mechanically unstable and do not discuss their elastic properties further.

Table 2 Elastic constants (C_{11}, C_{12} and C_{44}) and bulk modulus (B, in GPa) for γ-carbides $M_{23}C_6$ and mono-carbides MC in comparison with available data.

carbide	C_{11}	C_{12}
$Ru_{23}C_6$	416	256
RuC	521 (603[a]; 488/605[b])	230 (240[a]; 227/252[b])
$Rh_{23}C_6$	318	220
RhC	439 (425[c])	204 (251[c])
$Pd_{23}C_6$	257	153
PdC	276 (376[c]; 297[d]; 236[e])	181 (173[c]; 176[d]; 263[e])
$Os_{23}C_6$	440	218
OsC	543 (533[f])	271 (266[f])
$Ir_{23}C_6$	375	246
IrC	439 (486[f])	257 (247[f])
$Pt_{23}C_6$	273	225
PtC	259 (314[c]; 277[d]; 431[g]; 474[h]; 370[i]; 252[j]; 277[f])	254 (257[c]; 256[d]; 368b[g]; 214[h]; 283[i]; 271[j]; 256[f])
carbide	C_{44}	B
$Ru_{23}C_6$	42	309
RuC	11 (11[a]; 21.6/0.9[b])	327 (362[a])
$Rh_{23}C_6$	43	253
RhC	<0 (43[c])	282 (309[c])
$Pd_{23}C_6$	21	188
PdC	40 (56[c]; 44[d]; 20[e])	213 (241[c]; 217[d]; 254[e])
$Os_{23}C_6$	<0	292
OsC	<0 (<0[f])	361 (355[f])
$Ir_{23}C_6$	35	289
IrC	<0 (<0[f])	318 (236[f])
$Pt_{23}C_6$	<0	241
PtC	49 (24[c]; 52[d]; 66[g]; 56[h]; 50[i]; 55[j]; 52[f])	257 (276[c]; 264[d]; 389[g]; 301[h]; 282[i]; 257[j]; 263[f])

Available results are given in parentheses.
[a]Ref [7], FP-LMTO;
[b]Ref [12], LAPW-GGA/PW-LDA;
[c]Ref [13], FLAPW-GGA;
[d]Ref. [12], PW-GGA;
[e]Ref [40], FP-LMTO;
[f]Ref. [39], CASTEP;
[g]Ref. [35], LDA;
[h]Ref. [36], FP-LMTO;
[i]Ref. [37], DFT-GGA;
[j]Ref. [38], LDA.

By using the calculated constants C_{ij} we can estimate the elastic moduli – the bulk modulus (B) and the shear modulus (G) within Voigt (V), Reuss (R), and Voigt–Reuss–Hill (VRH) approximations for polycrystalline species as:

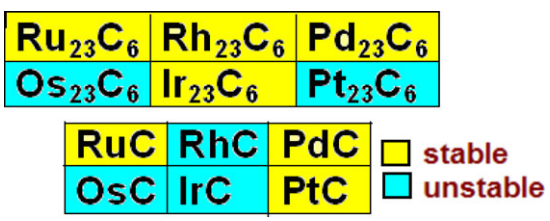

Figure 3 Mechanically stable and unstable $M_{23}C_6$ and MC carbides according to the Born's criterion.

$B_{V,R,VRH} = (C_{11} + 2C_{12})/3$; $G_V = (C_{11} - C_{12} + 3C_{44})/5$; $G_R = 5(C_{11} - C_{12})C_{44}/\{4C_{44} + 3(C_{11} - C_{12})\}$ and $G_{VRH} = G = (G_V + G_R)/2$, as well as compressibility $\beta = 1/B$. Besides, the average Young's modulus (Y) and the Poisson's ratio (ν) were estimated as $Y = 9B/\{1 + (3B/G)\}$ and $\nu = (3B - 2G)/2(3B + G)$.

These elastic parameters are shown in Tables 2 and 3. For the MC carbides, the calculated values of B are in good agreement with the previous theoretical predictions, Table 2. We found that monocarbides should have larger bulk moduli than $M_{23}C_6$, while for shear moduli such a trend is not observed. Among mechanically stable carbides, the ruthenium carbides ($Ru_{23}C_6$ and RuC) demonstrate the largest bulk and shear moduli.

For the majority of carbides, $B > G' > G$, i.e., the shear modulus G is a parameter limiting the mechanical stability of

Table 3 Compressibility (β, in GPa^{-1}), shear modulus (G, in GPa), Pugh's criterion (G/B), tetragonal shear modulus (G', in GPa), Young's modulus (Y, in GPa), Poisson's ratio (ν), Cauchy pressure (CP, in GPa), and elastic anisotropy indexes (A, A^U, and A_G) for mechanically stable $M_{23}C_6$ and MC carbides.

carbide	β	G_V[a]	G_R[a]
$Ru_{23}C_6$	0.00324	57	51.8
RuC	0.00306	64.8	17.5
$Rh_{23}C_6$	0.00395	45.4	45.2
$Pd_{23}C_6$	0.00532	33.4	27.6
PdC	0.00470	43.0	40.3
$Ir_{23}C_6$	0.00346	46.8	42.8
PtC	0.00389	30.4	5.8
carbide	Y	ν	CP
$Ru_{23}C_6$	154.5	0.417	214
RuC	118.7	0.440	220
$Rh_{23}C_6$	135.9	0.416	177
$Pd_{23}C_6$	86.8	0.423	132
PdC	116.9	0.408	141
$Ir_{23}C_6$	127.5	0.426	211
PtC	53.1	0.466	205
carbide	G[a]	G/B	G'
$Ru_{23}C_6$	54.4	0.176	80
RuC	41.2	0.126	146
$Rh_{23}C_6$	45.3	0.179	49
$Pd_{23}C_6$	30.5	0.162	52
PdC	41.6	0.195	48
$Ir_{23}C_6$	44.8	0.155	65
PtC	18.1	0.070	3
carbide	A	A^U	A_G
$Ru_{23}C_6$	0.525	0.50	4.8
RuC	0.076	13.5	57.5
$Rh_{23}C_6$	0.878	0.02	0.2
$Pd_{23}C_6$	0.404	1.05	9.5
PdC	0.842	0.33	3.2
$Ir_{23}C_6$	0.543	0.47	4.5
PtC	19.600	21.2	67.9

[a]As obtained within Voigt (G_V), Reuss (G_R), and Voigt–Reuss–Hill (G) approximations.

these materials. The exception is PtC, for which $B > G > G'$. The highest Young's modulus, which is a measure of stiffness, suggests that $Ru_{23}C_6$ and RuC are the stiffest compounds among the considered $M_{23}C_6$ and MC phases, respectively.

The Poisson's ratio (ν) is small for brittle covalent materials, whereas for ductile metallic-like materials ν is typically 0.33 [42]. In our case this parameter varies from 0.408 (for PdC) to 0.466 (for PtC) and from 0.416 (for $Rh_{23}C_6$) to 0.426 (for $Ir_{23}C_6$) that testifies to the metallicity of all these carbides. In addition, a negative Cauchy pressure $CP = (C_{12} - C_{44})$ takes place for covalent materials with strong directional bonds, whereas the Cauchy pressure is positive for metallic-like systems. We obtained that $CP > 0$ for all the carbides (Table 3), which points to weak covalent M–C bonds in these carbides.

The brittle/ductile behavior is an important mechanical property of materials, which is closely related to their reversible compressive deformation and fracture ability. One of the most widely used malleability measures of materials is the Pugh's criterion (G/B ratio [43]); namely, if $G/B < 0.57$, a material behaves in a ductile manner, and vice versa, if $G/B > 0.57$, a material demonstrates brittleness. According to this criterion, all the studied carbides should be ductile (Table 3).

Elastic anisotropy of crystals has an important implication since it correlates with the possibility to induce microcracks in materials. There are different approaches to estimate the elastic anisotropy of crystals, see review [16]. For cubic crystals, the most widely used parameter is the so-called Zener anisotropy index [44] $A = 2C_{44}/(C_{11} - C_{12})$. For isotropic crystals $A = 1$, while values smaller or greater than unity measure the degree of elastic anisotropy. For polycrystalline materials the universal anisotropy index [45] is defined as $A^U = 5G_V/G_R + B_V/B_R - 6$; for isotropic crystals $A^U = 0$, whereas the deviations of A^U from zero define the extent of crystal anisotropy. Additionally, using the model [46], we estimated elastic anisotropy (in percents) in shear (A_G) as $A_G = (G_V - G_R)/(G_V + G_R)$.

The calculated results (Table 3) indicate that among $M_{23}C_6$ carbides the smallest anisotropy should be expected for $Rh_{23}C_6$, whereas $Pd_{23}C_6$ should have the maximal anisotropy. Among the mono-carbides, PtC and PdC should demonstrate the maximal and minimal elastic anisotropy, respectively.

Finally, we tried to estimate the Vickers hardness (H_V), which is one of the important properties of materials determining often their technological and industrial applications. For this purpose, the bulk, shear, and Young's moduli as possible qualitative predictors of hardness were used within three known correlations [47–49]:

$$H_V = 0.0963B, \quad (1)$$

$$H_V = 0.1769G - 2.899, \quad (2)$$

$$H_V = 0.0608Y. \quad (3)$$

The calculated H_V and other available estimations of the Vickers hardness are shown in Fig. 4. We observe that these

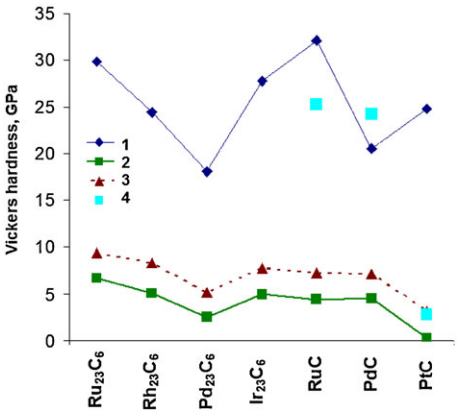

Figure 4 The Vickers hardness H_V for $M_{23}C_6$ and MC carbides as obtained within semi-empirical relationships $H_V \sim B$ (1); $H_V \sim G$ (2); $H_V \sim Y$ (3) in comparison with other theoretical estimations (4).

relationships are quite suitable approximations, which enable rough numerical evaluations of the main trends in the Vickers hardness for $M_{23}C_6$ from their elastic parameters. The obtained results suggest that $Pd_{23}C_6$ and $Ru_{23}C_6$ should have the minimal and maximal values of H_V among the considered $M_{23}C_6$ phases, but their values calculated within various models differ essentially. For the MC carbides, such correlations are absent. We note that hardness and elastic moduli are conceptually different parameters [16, 50].

The elastic moduli are related to elastic (*reversible*) deformations of crystals, whereas the hardness is a macroscopic parameter, which depends strongly on plastic (*irreversible*) deformation. Hardness is characterized experimentally by indentation, and it is governed by many factors of intrinsic (bond strength, cohesive energy, and crystal structure) and extrinsic (defects, stress fields, morphology, etc.) origin. Besides, it is well-known that hardness also depends on the methods of measurement, temperature, etc. Thus, no "universal" relationships between the Vickers hardness and elastic moduli may be expected, and the most suitable correlations need to be determined for each class of materials [16, 51]. Nevertheless, one can suggest that the correlations (2) and (3) are more appropriate for the prediction of hardness, which being a measure of plastic deformation, depends on shear stress and stress–strain relationship.

3.4 Electronic properties The total densities of states (DOS) for $M_{23}C_6$ and MC phases, as well as for the corresponding simple metals are shown in Fig. 5. All carbides exhibit non-zero densities of states at the Fermi level, $N(E_F)$, i.e., these phases should have metallic-like conductivity. For mono-carbides MC, the valence states are strictly divided into three main subbands (I–III, as labeled in Fig. 5 for RuC). The lowest states from -14 to -11 eV (subband I) come mainly from the C 2s states and the DOS's from -8 to -3 eV below the Fermi level, E_F (subband II) are

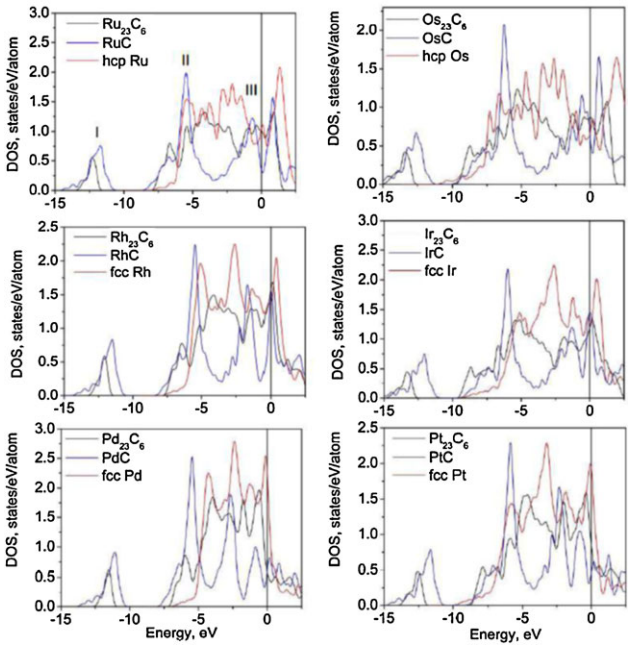

Figure 5 Total densities of states for $M_{23}C_6$ and MC carbides and for metals: M = Ru, Rh, Pd, Os, Ir, and Pt. The Fermi level $E_F = 0$ eV.

due to the C 2p and M d states, respectively. The bands from −3 eV up to E_F (subband III) are formed mainly by the M d states.

Other mono-carbides have similar three-peak DOS curves, which agree well with the previous band structure calculations [6–15].

There is a sharp minimum in the density of states between subbands II and III above −5 eV. It is well-known that the cohesive properties of mono-carbides are explained in terms of the band filling. For the most stable transition metal carbides (TiC, ZrC), the Fermi level falls in the pseudogap, where the bonding states are fully occupied and the antibonding states are empty. The additional valence electrons result in the shift of E_F and in the occupation of antibonding states, which corresponds to the lowering of cohesive properties and stability like for mono-carbides of platinum metals.

The densities of states for $M_{23}C_6$ look as being intermediate between DOS for the corresponding mono-carbide and pure metal. The lowest energy valence band narrows in $M_{23}C_6$ because of the reduced contribution of C 2s states, and the main difference in DOS for $M_{23}C_6$ versus MC is a broad peak in the region from −5.5 to −3 eV for $M_{23}C_6$, which is also present in elemental metals. This peak is formed mainly by the M d states, and comes from the direct d–d bonding of non-equivalent *M*1–*M*4 atoms. Thus, we can suggest that the stabilization of γ-carbides versus mono-carbides should be due to additional direct M–M interactions, which are absent in MC, but arise in $M_{23}C_6$.

Table 4 Total density of states at the Fermi level, $N(E_F)$ (states/eV/atom) for $M_{23}C_6$, MC and the corresponding metals M (M = Ru, Rh, Pd, Os, Ir, and Pt).

system	$N(E_F)$	system	$N(E_F)$
$Ru_{23}C_6$	1.01	$Os_{23}C_6$	0.86
RuC	0.34	OsC	0.61
hcp Ru	1.04	hcp Os	0.65
$Rh_{23}C_6$	1.58	$Ir_{23}C_6$	1.19
RhC	1.53	IrC	1.44
fcc Rh	1.39	fcc Ir	1.27
$Pd_{23}C_6$	0.58	$Pt_{23}C_6$	0.84
PdC	0.61	PtC	0.46
fcc Pd	2.29	fcc Pt	1.93

For $M_{23}C_6$ carbides, $N(E_F)$ changes non-monotonically with the number of valence electrons and the maximum is observed for $Rh_{23}C_6$ ($Ir_{23}C_6$), while the minimum – for $Pd_{23}C_6$ ($Pt_{23}C_6$), Table 4.

A similar parabolic dependence of $N(E_F)$ was found also for the mono-carbides, where the maximum $N(E_F)$ occurs for RhC and IrC, whereas the minimum value was found for RuC and PtC. However, $N(E_F)$ increases over the late transition metal series. The maximum of $N(E_F)$ corresponds to the Fermi level at the high M d-like DOS peak (ruthenium and iridium carbides), and a smaller or larger number of electrons results in a decrease of $N(E_F)$ and its parabolic dependence, Fig. 5. For elemental metals, the M d-like DOS peak is shifted to the high energies and the upper edge of the valence d band is occupied only for the late transition metals (Pd and Pt), where E_F falls at this high peak. As a result, $N(E_F)$ monotonically increases with an increase of the number of d electrons.

4 Conclusions Using first-principles calculations we studied the structural, elastic, and electronic properties of $M_{23}C_6$ and MC carbides, where M is the late transition metals (M = Ru, Rh, Pd, Os, Ir, or Pt.). We demonstrate that the formation of $M_{23}C_6$ phases is energetically more favorable as compared with the mono-carbides. The elastic constants and other elastic characteristics (bulk modulus *B*, shear modulus *G*, Young's modulus *E*, Poisson's ratio *ν*, elastic anisotropy parameters, and Vickers hardness) were estimated and compared for these carbides. It should be expected that $Ru_{23}C_6$, $Rh_{23}C_6$, $Pd_{23}C_6$, and $Ir_{23}C_6$, as well as RuC, PdC, and PtC are mechanically stable carbides. We predict that the ruthenium carbides ($Ru_{23}C_6$ and RuC) should have the largest elastic moduli and they are the stiffest compounds among the considered carbides. The lowest formation energy was obtained for $Ru_{23}C_6$, which should demonstrate the highest Vickers hardness and a small elastic anisotropy. The calculated densities of states show stronger M–M interactions in $M_{23}C_6$, which are responsible for the stabilization of $M_{23}C_6$ relative to MC carbides.

Acknowledgement The authors acknowledge the support from the RFBR, grant #12-03-00038-a.

References

[1] E. K. Storms, The Refractory Carbides (Academic Press, New York, 1967).
[2] L. E. Toth, Transition Metal Carbides and Nitrides (Academic Press, New York, 1971).
[3] S. Ono, T. Kikegawa, and Y. Ohishi, Solid State Commun. **133**, 55 (2005).
[4] A. L. Ivanovskii, Russ. Chem. Rev. **78**, 303 (2009).
[5] A. Friedrich, B. Winkler, E. A. Juarez-Arellano, and L. Bayarjargal, Materials **4**, 1648 (2011).
[6] Z. S. Zhao, M. Wang, L. Cui, J. L. He, D. L. Yu, and Y. J. Tian, J. Phys. Chem. C **114**, 9961 (2009).
[7] B. Abidri, M. Rabah, D. Rached, H. Baltache, H. Rached, I. Merzoug, and S. Djili, J. Phys. Chem. Solids **71**, 1780 (2010).
[8] Z. S. Zhao, L. F. Xu, M. Wang, L. Cui, L. M. Wang, J. L. He, Z. Y. Liu, and Y. J. Tian, Phys. Status Solidi RRL **4**, 230 (2010).
[9] H. R. Soni, S. K. Gupta, and P. K. Jha, Physica B **406**, 3556 (2010).
[10] V. Mankad, N. Rathod, S. D. Gupta, S. K. Gupta, and P. K. Jha, Mater. Chem. Phys. **129**, 816 (2011).
[11] K. K. Korir, G. O. Amolo, N. W. Makau, and D. P. Joubert, Diamond Relat. Mater. **20**, 157 (2011).
[12] C. Z. Fan, S. Y. Zeng, Z. J. Zhan, R. P. Liu, W. K. Wang, P. Zhang, and Y. G. Yao, Appl. Phys. Lett. **89**, 071913 (2006).
[13] V. V. Bannikov, I. R. Shein, and A. L. Ivanovskii, J. Phys. Chem. Solids **71**, 803 (2010).
[14] L. Li, Mod. Phys. Lett. **22**, 2937 (2008).
[15] M. Zhang, M. Wang, T. Cui, Y. M. Ma, Y. L. Niu, and G. T. Zou, J. Phys. Chem. Solids **69**, 2096 (2008).
[16] A. L. Ivanovskii, Prog. Mater. Sci. **57**, 184 (2012).
[17] X. P. Du and Y. X. Wang, J. Appl. Phys. **107**, 053506 (2010).
[18] X. A. Li, X. P. Du, and Y. X. Wang, J. Phys. Chem. C **115**, 6948 (2011).
[19] H. Pierson, Handbook of Refractory Carbides and Nitrides: Properties, Characteristics and Applications (Noyes Publications, Westwood, NJ, 1996).
[20] S. T. Oyama (ed.), The Chemistry of Transition Metal Carbides and Nitrides (Blackie Academic and Professional, London, 1996).
[21] V. V. Bannikov, I. R. Shein, and A. L. Ivanovskii, Phys. Status Solidi RRL **3**, 218 (2009).
[22] A. L. Bowman, G. D. Arnold, E. K. Storms, and N. G. Nereson, Acta Crystallogr. B **28**, 3102 (1997).
[23] C. M. Fang, M. A. van Huis, M. H. F. Sluiter, and H. W. Zandbergen, Acta Mater. **58**, 2968 (2010).
[24] G. Kresse and D. Joubert, Phys. Rev. B **59**, 1758 (1999).
[25] G. Kresse and J. Furthmuller, Phys. Rev. B **54**, 11169 (1996).
[26] J. P. Perdew, S. Burke, and M. Ernzerhof, Phys. Rev. Lett. **77**, 3865 (1996).
[27] G. Kresse, M. Marsman, and J. Furthmuller, VASP the GUIDE (Universität Wien, Austria, 2012).
[28] Y. Le Page, and P. Saxe, Phys. Rev. B **65**, 104104 (2002).
[29] A. L. Ivanovskii, N. I. Medvedeva, and J. E. Medvedeva, Mendeleev Commun. **4**, 129 (1998).
[30] A. L. Ivanovskii, N. I. Medvedeva, G. P. Shveikin, Y. Y. Medvedeva, and A. E. Nikiforov, Metallofiz. Novejsh. Tekhnol. **20**, 41 (1998).
[31] A. L. Ivanovskii, N. I. Medvedeva, and Y. Y. Medvedeva, Metallofiz. Novejsh. Tekhnol. **21**, 19 (1999).
[32] A. L. Ivanovskii and N. I. Medvedeva, Russ. J. Inorg. Chem. **45**, 1234 (2000).
[33] N. I. Medvedeva, J. E. Medvedeva, A. L. Ivanovskii, V. G. Zubkov, and A. J. Freeman, JETP Lett. **73**, 336 (2001).
[34] N. I. Medvedeva, L. E. Kar'kina, and A. L. Ivanovskii, Phys. Met. Metallogr. **96**, 452 (2003).
[35] E. Deligoz, Y. O. Ciftci, P. T. Jochym, and K. Colakoglu, Mater. Chem. Phys. **111**, 29 (2008).
[36] M. Rabah, D. Rached, M. Ameri, R. Khenata, A. Zenati, and N. Moulay, J. Phys. Chem. Solids **69**, 2907 (2008).
[37] F. Peng, H. Z. Fu, and X. D. Yang, Solid State Commun. **145**, 91 (2008).
[38] L. Y. Li, W. Yu, and C. Q. Jin, J. Phys.: Condens. Matter **17**, 5965 (2005).
[39] J. Yang and F. Gao, Physica B **407**, 3527 (2012).
[40] M. Rabah, S. Benalia, D. Rached, B. Abidri, H. Rached, and G. Vergoten, Comput. Mater. Sci. **48**, 556 (2010).
[41] M. Born and K. Huang, Dynamical Theory of Crystal Lattices (Clarendon, Oxford, 1956).
[42] J. Haines, J. M. Leger, and G. Bocquillon, Annu. Rev. Mater. Res. **31**, 1 (2001).
[43] S. F. Pugh, Philos. Magn. **45**, 823 (1953).
[44] C. Zener, Elasticity and Anelasticity of Metals (University of Chicago, Chicago, 1948).
[45] S. I. Ranganathan and M. Ostoja-Starzewshi, Phys. Rev. Lett. **101**, 055504 (2008).
[46] H. Chung and W. R. Buessem, in: Anisotropy in Single Crystal Refractory Compound, edited by F. M. Vahldiek and S. A. Mersol (Plenum Press, New York, 1968), p. 217.
[47] D. M. Teter, MRS Bull. **23**, 22 (1998).
[48] X. Jiang, J. Zhao, A. Wu, Y. Bai, and X. J. Jiang, J. Phys.: Condens. Matter **22**, 315503 (2010).
[49] X. Jiang, J. Zhao, and X. Jiang, Comput. Mater. Sci. **50**, 2287 (2011).
[50] J. J. Gilman, Chemistry and Physics of Mechanical Hardness (Wiley, Hoboken, NJ, 2009).
[51] A. L. Ivanovskii, Int. J. Refract. Met. Hard Mater. **36**, 179 (2013).

